2,4-Dichlorophenol Degradation Using *Streptomyces viridosporus* T7A Lignin Peroxidase

Dennis C. Yee and Thomas K. Wood*

Department of Chemical and Biochemical Engineering, University of California, Irvine, California 92697-2575

The *Streptomyces viridosporus* T7A bacterium produces the extracellular lignin peroxidase ALiP-P3. The ALiP-P3-catalyzed oxidation of 2,4-dichlorophenol (DCP) was examined to understand its kinetic behavior. Initial rate data of the oxidation of DCP were obtained by a spectrophotometric peroxidase assay, and the kinetics were best modeled with a random-binding bireactant system, which differs from the ping-pong bireactant system that is typically used for horseradish peroxidase and lignin peroxidase from the fungus *Phanerochaete chrysosporium*, and suggests that either DCP or H_2O_2 may bind first to ALiP-P3. Chloride ion measurements indicate that 16% of the reacted DCP was fully dechlorinated by ALiP-P3. Chemical ionization mass spectrometry was also utilized to identify the DCP degradation product as a hydrophobic chlorinated dimer of mass 322.

Introduction

Chlorophenols, such as 2,4-dichlorophenol (DCP), are used extensively in the manufacture of pesticides, herbicides, and wood preservatives (Kroschwitz, 1993; Syracuse Research Corp., 1992). DCP was the most produced chlorophenol in 1989 (Kroschwitz, 1993) and can be found in the environment in degraded herbicides, sawmills, wood waste incinerators, and hazardous waste sites (Syracuse Research Corp., 1992; World Health Organization, 1989). DCP can cause death, respiratory failure, bone marrow atrophy, and skin damage in animals (Kintz et al., 1992; Syracuse Research Corp., 1992) and confers a distasteful taste and odor to food and water (Buikema et al., 1979). Because of its manufacture in large quantities, animal effects, and organoleptic qualities, DCP is an EPA priority pollutant (Wentz, 1989) identified in hazardous waste sites identified on the National Priorities List (Syracuse Research Corp., 1992).

S. viridosporus T7A is a Gram-positive bacterium that produces an extracellular peroxidase, ALiP-P3, that catalyzes the oxidation of DCP. ALiP-P3 is implicated in the lignin-degrading system of *S. viridosporus* T7A and catalyzes the production of a major lignin degradation product, a water-soluble, acid-precipitable polymeric lignin (Borgmeyer and Crawford, 1985; Crawford et al., 1984; Ramachandra et al., 1987). The ALiP-P3 enzyme is one of four lignin peroxidase isoforms produced by *S. viridosporus* T7A, and it has the greatest known substrate range (Ramachandra et al., 1988; Spiker et al., 1992). The ability of ALiP-P3 to catalyze the degradation of several recalcitrant lignin bonds in the presence of H_2O_2, including 1,2-diarylpropane (β-1) and arylglycerol-β-aryl ether (β-O-4) bonds (Ramachandra et al., 1988), suggests that it may be used to degrade recalcitrant compounds such as DCP and other chlorophenols.

Peroxidases catalyze the oxidation of aromatic compounds to form free radical products that may react further. The generally accepted reaction mechanism, initially developed for yeast cytochrome *c* peroxidase, is shown in eq 1 (Anni and Yonetani, 1992).

$$\mathrm{LiP[Fe^{III}] + H_2O_2 \rightarrow LiPI[\underline{Fe^{IV}{=}OR^{\bullet}}] + H_2O}$$

$$\mathrm{LiPI[\underline{Fe^{IV}{=}OR^{\bullet}}] + AH_2 \rightarrow LiPII[\underline{Fe^{IV}{=}OR}] + HA^{\bullet} + H^{+}} \quad (1)$$

$$\mathrm{LiPII[\underline{Fe^{IV}{=}OR}] + AH_2 \rightarrow LiP[Fe^{III}] + HA^{\bullet} + OH^{-}}$$

$$\mathrm{2AH_2 + H_2O_2 \xrightarrow{LiP} 2HA^{\bullet} + 2H_2O} \quad (2)$$

The activation of the native peroxidase (indicated as LiP) occurs by a transfer of an oxygen atom (with six valence electrons) to the heme porphyrin. Compound I, or LiPI, is consequently formed by an intramolecular arrangement of the electrons in the porphyrin ring. In the yeast cytochrome *c* peroxidase, the formation of compound I occurs during a concommitant change of Fe(III) to Fe(IV) heme oxidation state and formation of a porphyrin π-cation radical. A stable compound I is formed after the cation radical dismutates to a free radical on a nearby protein residue (Anni and Yonetani, 1992). Therefore, the stable compound I possesses two oxidizing equivalents: one in the protein radical and the other in the Fe(IV)=O complex.

The formation of LiPII (or compound II) occurs through the oxidation of a reducing substrate by LiPI. For yeast cytochrome *c* peroxidase, an electron is transferred from the substrate to the protein free radical. The remaining oxidizing equivalent in the Fe(IV)=O complex enables the oxidation of a second substrate by LiPII, yielding a free radical product, releasing a proton and the heme-bound oxygen atom, and returning the enzyme to its native state. Therefore, the overall reaction (eq 2) involves the reaction of two aromatic molecules with H_2O_2 and LiP to form two free radical aromatic products and water. A variety of NMR, EPR, and Mossbauer spectroscopy studies have shown that horseradish peroxidase follows a similar activation and reaction mechanism. Although no such studies have been performed with the *S. viridosporus T7A* lignin peroxidase, studies of the *P. chrysosporium* lignin peroxidase also indicate that peroxidase intermediates exist which are similar to those of the cytochrome *c* and horseradish peroxidases.

* Corresponding author. Telephone: (714) 824-3147. FAX: (714) 824-2541. E-mail: TKWOOD@UCI.EDU.

S8756-7938(96)00091-4 CCC: $14.00

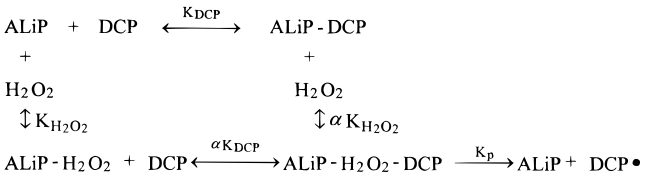

Figure 1. Random Bi Bi kinetic model. K_{DCP} represents the binding constant of DCP to ALiP-P3. $K_{H_2O_2}$ represents the binding constant of H_2O_2 to ALiP-P3. α represents the change in binding affinity of the enzyme to one substrate that occurs after the first substrate binds to the enzyme.

An enzyme reaction involving two substrates generally can be described by one of three models: the random-binding, bireactant (Bi Bi), the ordered Bi Bi, or the ping-pong Bi Bi kinetic model. The kinetic system of both lignin peroxidase from the white rot fungus, *P. chrysosporium*, and horseradish peroxidase have been modeled previously with the ping-pong bireactant (Bi Bi) kinetic system (Everse et al., 1991; Hu et al., 1993; Segel, 1975). This kinetic model assumes that the peroxidase binds to H_2O_2 first, forming an enzyme with two additional oxidation equivalents. This modified enzyme can then bind and react with an aromatic substrate, such as DCP, to form a free radical product.

Whereas both the ordered Bi Bi and the ping-pong Bi Bi models assume that the native ALiP-P3 must react first with H_2O_2 before it can bind and react with DCP, the random-binding bireactant model assumes that an ALiP-P3−DCP−H_2O_2 enzyme complex is formed by any order of substrate binding (Figure 1). Additionally, the binding constant, α, is assumed to be the same for binding of the enzyme to either DCP or H_2O_2. The ping-pong and random-binding models both assume that all binding steps are at equilibrium and that only the AH• product formation steps are rate-limiting.

The derived rate equation for the random bireactant kinetic model is shown in eq 3 (Segel, 1975). The binding

$$V = \frac{V^*_{max}[H_2O_2][DCP]}{\alpha K_{DCP}K_{H_2O_2} + \alpha K_{H_2O_2}[DCP] + \alpha K_{DCP}[H_2O_2] + [H_2O_2][DCP]} \quad (3)$$

factor, α, represents the change in binding affinity of the enzyme to one substrate that occurs after the other substrate binds the enzyme. To determine the four kinetic parameters, V^*_{max}, K_{DCP}, $K_{H_2O_2}$, and α, the rate equation may be converted to the forms shown in eqs 4 and 5:

$$\frac{1}{V} = \frac{\alpha K_{H_2O_2}}{V^*_{max}}\left(1 + \frac{K_{DCP}}{[DCP]}\right)\frac{1}{[H_2O_2]} + \frac{1}{V^*_{max}}\left(1 + \frac{\alpha K_{DCP}}{[DCP]}\right) \quad (4)$$

$$\frac{1}{V} = \frac{\alpha K_{DCP}}{V^*_{max}}\left(1 + \frac{K_{H_2O_2}}{[H_2O_2]}\right)\frac{1}{[DCP]} + \frac{1}{V^*_{max}}\left(1 + \frac{\alpha K_{H_2O_2}}{[H_2O_2]}\right) \quad (5)$$

In these equations, the inverse of the apparent V_{max} is obtained by dividing the slope of either equation by αK (either $K_{H_2O_2}$ or K_{DCP}, as applicable).

An efficient bioreactor process that utilizes ALiP-P3 of *S. viridosporus* T7A must be designed with an understanding of DCP-degradation kinetics. Because H_2O_2 is required for catalytic activity, the effect of the H_2O_2 and DCP substrate concentrations on enzyme activity needs to be characterized. Furthermore, the degradation products of the ALiP-P3-catalyzed oxidation of DCP should be identified so that further degradation and/or processing can be considered.

Using the random bireactant model for the DCP degradation catalyzed by ALiP-P3, the kinetic rate constants were calculated and optimal concentrations of H_2O_2 were determined for maximum DCP removal. A cornstarch-based culture medium (DJMM) that was previously developed for *S. viridosporus* T7A was used to produce ALiP-P3 (Yee et al., 1996). In addition, preliminary results that attempt to identify and characterize the degradation products by measurement of chloride ions and mass spectrometry are reported.

Materials and Methods

Organism and Culture Conditions. *S. viridosporus* T7A (ATCC 39115) was supplied by Prof D. L. Crawford (University of Idaho, Moscow, ID) and cultivated at 30 °C in 50 mL of starch-containing DJMM, as described previously (Yee and Wood, 1996). The cultures were harvested for ALiP-P3 after 6 days, as described below.

Extracellular ALiP-P3 Isolation. The ALiP-P3-containing culture supernatant was separated from the cells by centrifugation of the *S. viridosporus* T7A cultures at 4 °C for 10 min at 18000*g* in a model J2-21 centrifuge (Beckman Industries, Inc., Palo Alto, CA). The supernatant was then saturated with NH_4SO_4 to 35% saturation and equilibrated by gentle stirring for 45 min at 4 °C. After equilibration, the solution was centrifuged at 4 °C for 15 min at 20000*g* and the supernatant was collected. A second precipitation cut was performed with the collected supernatant by increasing NH_4SO_4 from 35% to 75% saturation and equilibrating the solution for 45 min at 4 °C. The solution was centrifuged again at 4 °C for 15 min at 20000*g*. The precipitated protein pellet was resuspended to 75% of the initial culture supernatant volume with either 50 mM Tris-HCl (pH 8) buffer or 10 mM sodium phosphate (pH 7) buffer and dialyzed against 4 L of the same buffer overnight in a 10 000 MW dialysis membrane. The isolated crude ALiP-P3 preparation was stored at 4 °C when not used.

Peroxidase Assay. ALiP-P3 activity was determined spectrophotometrically from the initial rate of the ALiP-P3-catalyzed DCP degradation in which colored antipyrylquinonimine forms from DCP and 4-aminoantipyrene (AAP), as described previously (Yee et al., 1996). The ALiP-P3 activity was measured at varying initial DCP and H_2O_2 concentrations in a 1.0 mL aqueous assay mixture with final concentrations of 100 mM Tris-HCl buffer, pH 8.0 (Fisher Scientific, Tustin, CA), 8.0 mM AAP (Fisher), and 100 mL of ALiP-P3 crude enzyme preparation. Two sets of initial rate data were obtained using this peroxidase assay, with triplicate measurements for each data point. The first set was measured at a fixed DCP (Fisher) concentration (50, 100, 200, or 300 μM) while the initial H_2O_2 concentration (Fisher) was varied from 5 to 50 mM. The other set of data was measured at a fixed H_2O_2 concentration (10, 20, 30, or 40 mM) and initial DCP concentrations varied between 50 and 600 μM.

Chloride Ion Measurement. Chloride ions were measured spectrophotometrically with the procedure of Bergmann and Sanik (1957) by adding 200 μL of 0.25 M $Fe(NH_4)(SO_4)_2 \cdot 12H_2O$ in 9 M HNO_3 to 0.6 mL of the aqueous sample to be analyzed. After addition of 200 μL of $Hg(SCN)_2$, the mixture is developed for 10 min and the absorbance of the $Fe(SCN)^{2+}$ product at 460 nm is measured with a DU640 spectrophotometer (Beckman Instruments). The colored $Fe(SCN)^{2+}$ product and $HgCl_2$

are both formed as free chloride ions displace the thiocynate ion of $Hg(SCN)_2$.

The change in chloride ion concentration of triplicate, ALiP-P3-catalyzed DCP-degradation reactions was measured over time. The 10 mL degradation reaction contained 10 mM sodium phosphate buffer (pH 7), 5 mM DCP, and 5 mL of the isolated ALiP-P3 preparation described previously. After the reaction was initiated with 5 mM H_2O_2, the samples were shaken at 250 rpm in a 30 °C orbital air bath, and the chloride ion concentration of 600 μL aliquots was measured every 30 min. Two sets of negative controls, each consisting of duplicate vials, were also run to measure the chloride ion generated from H_2O_2 alone and the chloride ion generated from ALiP-P3 without H_2O_2. In each of the negative controls, water was substituted for the removed reagent.

The percent of dechlorinated DCP was calculated by assuming that the dechlorination of each DCP molecule resulted in the release of two chloride ions. The dechlorinated DCP was then determined as the percentage of DCP that reacted in the ALiP-P3 enzyme assay described in the previous section.

Gas Chromatography. The ALiP-P3-catalyzed, DCP degradation rates determined by the spectrophotometric assay were corroborated using GC measurements with isolated ALiP-P3 enzyme. A 25 mL DCP degradation reaction was conducted with ALiP-P3 isolated enzyme, 10 mM DCP, 50 mM Tris-HCl buffer (pH 8), and 250 mM H_2O_2. After stirring for 10 min at ambient temperature, 5 mL of the reaction mixture was removed, supplemented with 50 μmol of napthalene (Fisher) standard, and the solution was extracted with two aliquots of 5 mL of CH_2Cl_2. The CH_2Cl_2 extract was concentrated to 0.5 mL using a Kuderna−Danish apparatus (Fisher) heated with a 35 °C water bath. The extracted DCP in the 0.5 mL concentrate was derivatized with 35 μL of trifluoroacetic anhydride (Aldrich Chemical Co., Milwaukee, WI) and 15 μL of pyridine (Fisher). Negative controls (containing both DCP and H_2O_2 but lacking ALiP-P3) were similarly reacted and prepared.

The derivatized samples were analyzed by injecting a 1 μL sample into a 1% Supelcoport SP1240DA (100/120 mesh) packed column in a Varian 3600 GC (Varian Associates, Walnut Creek, CA). The column temperature was increased from 70 to 130 °C at 4 °C/min, while the injector and FID detector temperatures were 200 and 220 °C, respectively. DCP concentrations were determined from calibration curves generated by similarily measuring a range of known DCP concentrations (0.4−8 mM).

Mass Spectrometry. A preliminary analysis of the DCP degradation products was done with MS analysis by chemical ionization of an ALiP-P3-catalyzed DCP degradation reaction. A 20 mL reaction was conducted in a 60 mL serum vial containing 50 mM sodium phosphate buffer (pH 8), 5 mM DCP, and 10 mL of isolated ALiP-P3 preparation. The reaction was initiated by the addition of 5 mM H_2O_2 and shaken for 1 h in an orbital air bath at 250 rpm at 30 °C. The reacted sample was isolated by either methylene chloride extraction or evaporation of the remaining water. Extraction of a 10 mL aliquot of the degradation reaction was performed with two 10 mL aliquots of methylene chloride, followed by evaporation of the methylene chloride to 0.2 mL under a vacuum. This concentrated sample was dried over anhydrous sodium sulfate and resuspended with methylene chloride to a 0.5 mL volume.

The organic-isolated sample was analyzed by chemical ionization (isobutane) mass spectrometry for the determination of the molecular mass of any isolated degradation products. The mass spectrometry analysis was conducted with an Autospec mass spectrometer (Fisons Instruments, Beverly, MA), initially at 25 °C and then increased to 330 °C with a 50 °C/min temperature ramp.

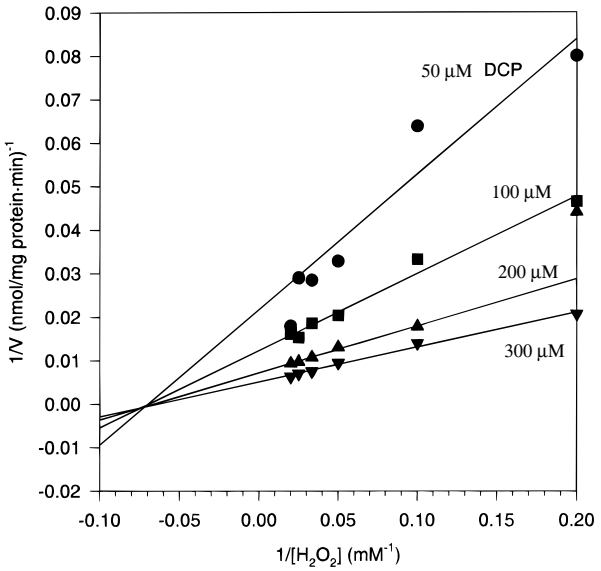

Figure 2. Initial plot of 1/rate vs $1/[H_2O_2]$ at fixed DCP concentrations of 50, 100, 200, and 300 μM. Data are the average of triplicate initial rate measurements.

Results

DCP-Degradation Kinetic Study. The random-binding nature of the bireactant kinetic model was suggested after plotting each set of initial rate data (Figures 2 and 3) as $1/V$ vs 1/[substrate]. Because the family of curves for fixed H_2O_2 plots do not intersect on the line represented by $1/[DCP] = 0$, a random-binding bireactant system is indicated, as opposed to an ordered Bi Bi system (in which the curves do intersect on $1/[DCP] = 0$) (Segel, 1975).

These results also indicate that the system is not a ping-pong bireactant system, which would result in parallel curves that do not intersect (Segel, 1975). From the initial plots (Figures 2 and 3), the *y* intercept of each curve yields the the apparent maximum initial rate. This may be replotted (Figure 4) so that the *y* intercept of the apparent maximum rate of a fixed DCP concentration plotted against the DCP concentration determines the maximum reaction rate, $V^*_{max} = 465.8$ nmol/(mg of protein·min). This maximum reaction rate obtained from the spectrophotometric assay was corroborated using a gas chromatograph assay where an initial rate of 539 nmol/(mg of protein·min) was found by measuring the disappearance of 10 mM DCP in 10 min with 250 mM H_2O_2 [a $V^*_{max} = 410$ nmol/(mg of protein·min) is predicted using the calculated kinetic constants at these substrate concentrations].

A second set of replots (plotting the slopes of the curves from Figure 2 or 3 vs the substrate concentration) may be used to obtain the binding constants (K) for DCP and H_2O_2 (Figures 5 and 6). The *x* intercepts of Figures 5 and 6 result in a $K_{DCP} = 372.2$ μM and $K_{H_2O_2} = 37.7$ mM. The factor α was then determined from the *y* intercept of Figure 6, giving $\alpha = 0.7$. These determined parameters are summarized in Table 1.

Additional initial rate data were obtained at fixed concentrations of either $[DCP] = 450$ μM or $[H_2O_2] = 50$ mM to test the ability of the determined kinetic parameters to predict the initial reaction rates at substrate ranges slightly outside of the conditions initially used to obtain those parameters. Figures 7 and 8 show that the

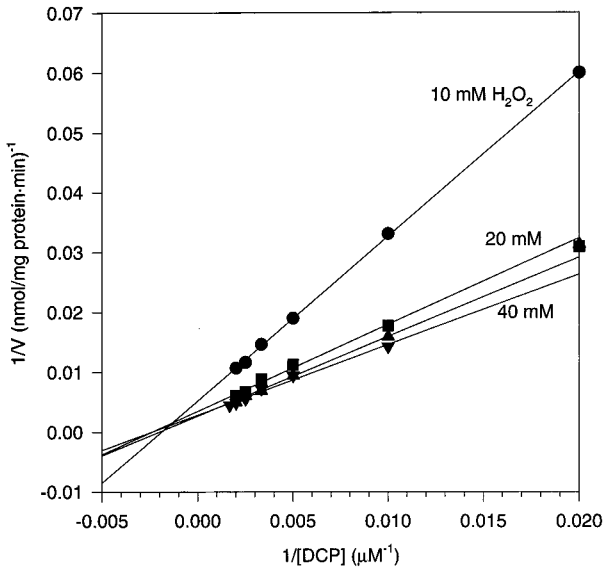

Figure 3. Initial plot of 1/rate vs 1/[DCP] at fixed H_2O_2 concentrations of 10, 20, 30, and 40 mM. Data are the average of triplicate initial rate measurements.

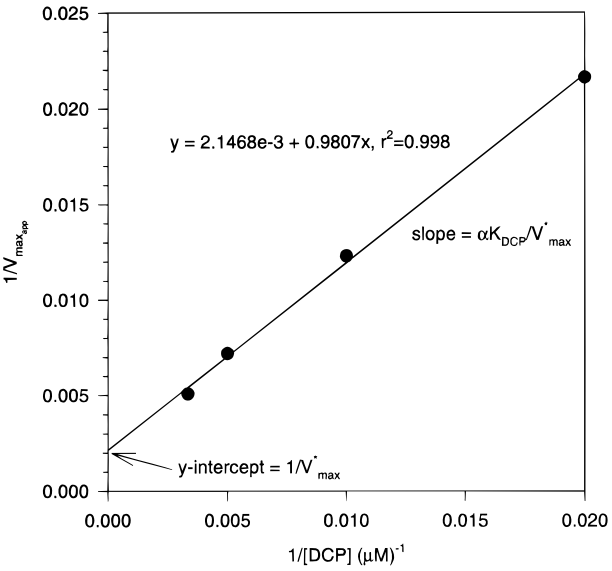

Figure 4. Plot of y intercepts (or apparent V_{max}, from Figure 2) vs 1/[DCP]. The V^*_{max} is determined from the y intercept of the line generated from a least-squares fit. The R^2 value represents correlation coefficient from least-squares fit of data.

trends followed by the actual rates are predicted by the random Bi Bi model with the calculated kinetic constants.

Chloride Ion Measurements. From the data in Figure 9, up to 68 μM chloride ions were generated from the ALiP-P3-catalyzed DCP oxidation reaction. If the dechlorination reaction is assumed to completely dechlorinate DCP and release two chloride ions from each molecule of DCP, then of the DCP that reacted with the AAP (as determined using the spectrophotometric peroxidase assay, data not shown), 16% of the reacted DCP was fully dechlorinated.

MS Analysis. To gain an understanding of the ALiP-P3-catalyzed DCP degradation products, the DCP reaction products were analyzed by mass spectrometry. The reaction products were isolated for analysis by the reaction mixture with methylene chloride. The spectra obtained from the organic-extracted sample (Figure 10) indicate two major ions. The predominant ion (m/z = 162) corresponds to DCP, while the second ion was initially identified with m/z = 324. Additional exact

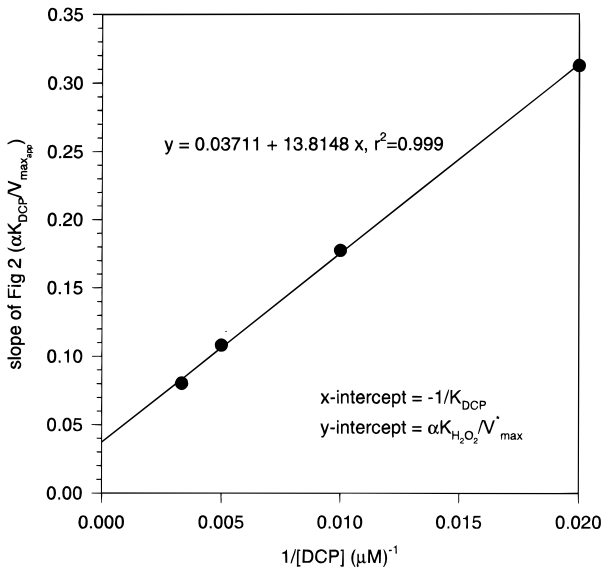

Figure 5. Plot of slopes (determined from Figure 2) vs 1/[DCP]. The factor K_{DCP} is determined from the x intercept of the line generated from a least-squares fit. The R^2 value represents correlation coefficient from least-squares fit of data.

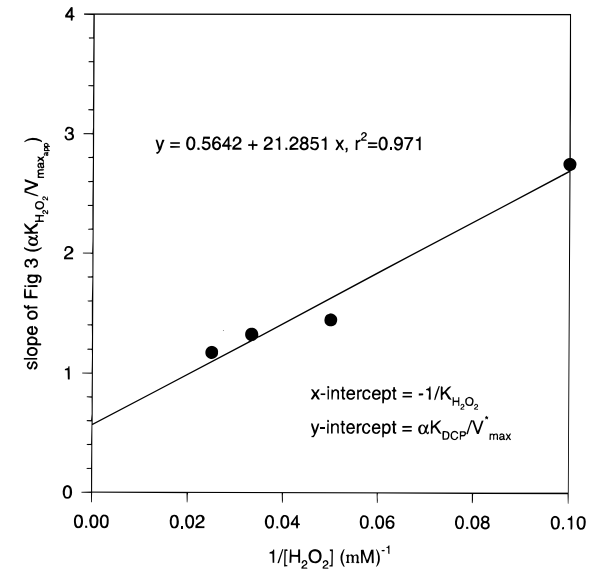

Figure 6. Plot of slopes (determined from Figure 3) vs 1/[H_2O_2]. The factors $K_{H_2O_2}$ and α are determined from the x and y intercepts of the line generated from a least-squares fit.

Table 1. Random Bireactant Kinetic Constants for the ALiP-P3-Catalyzed DCP Degradation as Determined from Initial Rate Data

kinetic constant	calculated value
α	0.7
V^*_{max} [nmol/(mg of protein·min)]	465.8
K_{DCP} (μM)	372
$K_{H_2O_2}$ (mM)	38

mass measurements of this second, unidentified ion yielded a molecular ion mass of 321.9117, which corresponds to a molecule with the empirical formula, $C_{12}H_6O_2Cl_4$. Figure 11 depicts a possible structure matching the empirical formula determined by mass spectroscopy and indicates that this compound most likely results from the condensation of free radical DCP, yielding a chlorinated product.

Since the chloride ion measurements show that 16% of the chloride ions were released, the mass spectra of partially dechlorinated compounds also would be expected. However, because minimal sample separation

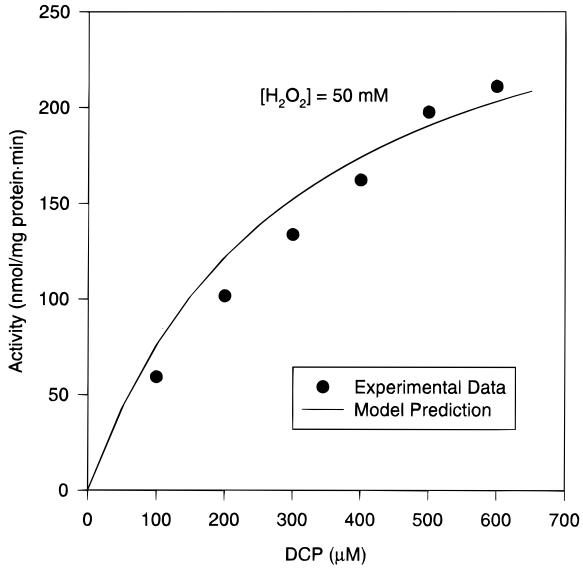

Figure 7. Test of kinetic parameters determined from initial rate data. The predicted initial rates are compared to the measured rates at a fixed H_2O_2 concentration of 50 mM.

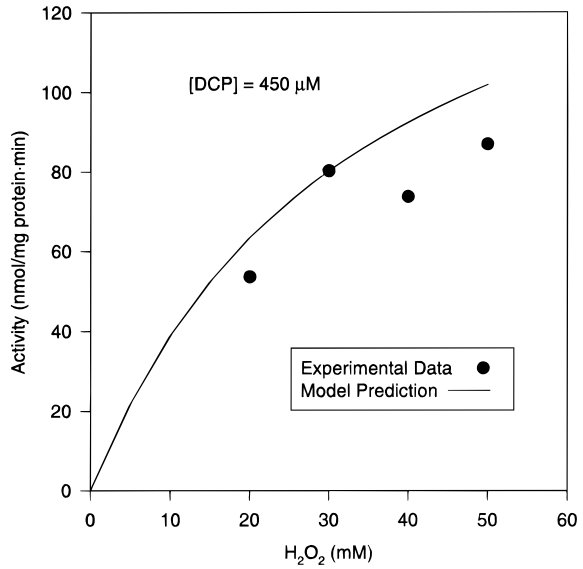

Figure 8. Test of kinetic parameters determined from initial rate data. The predicted initial rates are compared to the measured rates at a fixed DCP concentration of 450 μM.

was achieved by direct chemical ionization, less-chlorinated derivatives of $C_{12}H_6O_2Cl_4$ (that also may have been produced by the ALiP-P3 reaction) cannot be distinguished from the fragmentation ions generated by $C_{12}H_6O_2Cl_4$.

Discussion

The kinetics of the ALiP-P3 reaction which catalyze the oxidation of DCP was modeled using a random-binding bireactant system. This model differs from the ping-pong bireactant system used to describe the kinetics of horseradish peroxidase (Everse et al., 1991) and *P. chrysosporium* lignin peroxidase (Hu et al., 1993), which assumes that H_2O_2 must first bind and activate the enzyme before DCP binds. However, the model provided by the random bireactant system is a valid alternative that would still support the general peroxidase reaction mechanism since DCP oxidation still occurs only after H_2O_2 activation of ALiP-P3, except that the native enzyme may first bind to DCP and then obtain two oxidizing equivalents from the peroxide. It should be

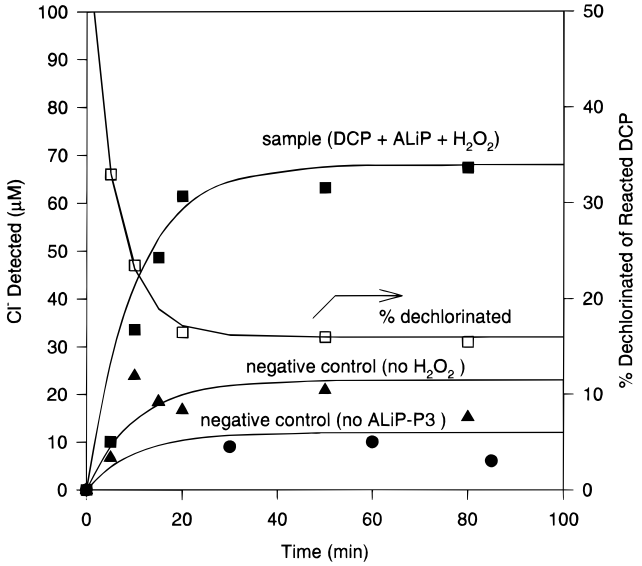

Figure 9. Chloride ions released during ALiP-P3-catalyzed DCP degradation. The data represent the average of triplicate samples. The percentage of reacted DCP that was fully dechlorinated is also shown.

noted that the hydrogen peroxide concentrations used in this study were at least 1−2 orders of magnitude higher than the peroxide concentrations used in previous studies (Andrawis et al., 1988; Hu et al., 1993) because the DCP degradation kinetics were modeled for conditions favorable to high DCP degradation rates, not for typical physiological conditions.

As shown by Hu *et al.* (1993) with *P. chrysosporium* lignin peroxidase, plots of inverse rates vs inverse [oxidized substrate], obtained at inhibiting H_2O_2 concentrations, would yield a similar trend as observed in this study. This phenomenon indicates that competitive inhibition of the peroxidase reaction occurs due to high H_2O_2 concentrations in which an inactive lignin peroxidase is formed upon reaction of active LiP with H_2O_2 (Wariishi and Gold, 1990). Nevertheless, the data presented in this study verify that the random bireactant model is an appropriate model since Figure 2 clearly shows that the initial rates were not measured under inhibitory H_2O_2 concentrations (i.e., the slopes are positive).

The inhibitory effect of H_2O_2 on enzyme activity and stability is one aspect of the enzyme kinetics which was not examined. This characterization of ALiP-P3 would be very important, particularly in the context of a sustained DCP degradation process. As previously mentioned, H_2O_2 at high concentrations exerts a negative effect on *P. chrysosporium* lignin peroxidase activity (Hu et al., 1993). Our own observations with ALiP-P3 also support these findings (unpublished data).

The kinetic parameter, α, of the random bireactant system is a measure of the change in the enzyme's binding affinity to one substrate after the other has formed an enzyme−substrate complex. The binding factor determined for ALiP-P3 ($\alpha = 0.7$) from this study indicates that, once DCP or H_2O_2 is bound to the enzyme, the affinity of the resulting complex for the remaining substrate is lower than that of the native enzyme. This lower affinity may be due to the fact that DCP is not the natural substrate of ALiP-P3.

The chloride ion results show that DCP is dechlorinated. The chloride is generated very early in the reaction (within 5 min) but does not appear to increase with the additional DCP that is oxidized, as shown by the peroxidase assay. One explanation for this unusual

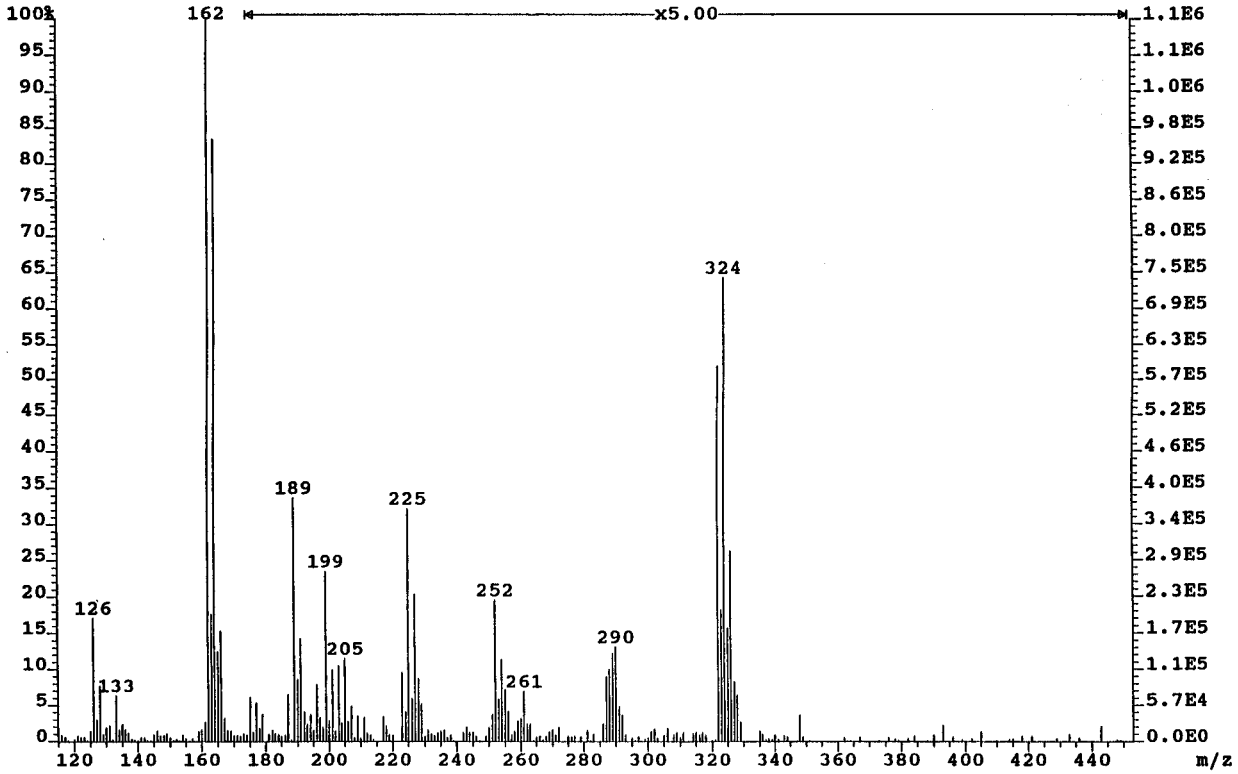

Figure 10. Mass spectra obtained from the organic-extracted ALiP-P3-catalyzed DCP-degradation sample.

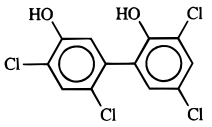

MW 321.9117

Figure 11. Possible structure of the product resulting from the ALiP-P3-catalyzed DCP-degradation reaction.

result may be that the two states of the activated peroxidase catalyze slightly different substrates. In addition to DCP, the initial H_2O_2-activated enzyme (ALiPI) may also catalyze the dechlorination of the oxidized DCP, whereas the second enzyme form (ALiPII) only catalyzes the oxidation of DCP. However, this hypothesis assumes that ALiPII does not return to its native state after reacting with DCP, but is changed to an inactive state.

The enzyme assay conducted with the chloride ion experiment shows that only 3.5% of the total DCP was reacted (determined spectrophotometrically by measuring the antipyrylquinonimine formed by reacting ALiP-P3 with DCP, H_2O_2, and AAP; data not shown). However, under these assay conditions, the reaction is enzyme limited, and we have observed that this extent of DCP reaction is highly dependent on the DCP concentration (unpublished results). However, because of low sensitivity and background interference inherent with the chloride ion measurement method used, a high initial DCP concentration was used to ensure the detection of significant levels of chloride ion above background. Further investigation is needed, therefore, to quantify the effect of both DCP and H_2O_2 on the extent of the ALiP-P3-catalyzed reaction.

The lignin peroxidase and manganese peroxidases of *P. chrysosporium* are believed to catalyze the oxidation of the hydroxyl group of DCP, by the above reaction mechanism, which then forms 2-chloro-1,4-benzoquinone (Valli and Gold, 1991). A variety of other microorganisms also degrade DCP with enzymes other than peroxidases. *Actinobacter*, *Pseudomonas cepacia*, and *Arthrobacter* species can degrade DCP to 3,5-dichlorocatechol using a 2,4-dichlorophenol hydroxylase (Bollag et al., 1968; Häggblom, 1990; Radjendirane et al., 1991). Whole cell cultures of *Streptomyces rochei* 303 also degrade DCP with an unidentified enzyme to 2,6-dichlorohydroquinol and chlorohydroquinol (Golovleva et al., 1992).

These preliminary mass spectrometry results indicate that ALiP-P3 catalyzes the formation of a DCP degradation product that is different from the quinones and dichlorocatechols observed from other microorganisms. However, using a phenol oxidase isolated from the fungus *Rhizoctonia praticola*, dimer products were identified by mass spectrometry with the same mass as the MW^+ 322 hydrophobic degradation product observed in this study (Liu et al., 1991; Minard et al., 1981). Although additional work is required to identify the dechlorinated reaction products, these results show that dimer products are predominantly formed and that ALiP-P3 catalyzes the oxidation of DCP by a random-binding bireactant enzyme system.

Acknowledgment

This study was supported by the National Science Foundation (Grant BES-9210619). We would like to thank Prof. Frank Evans (University of California, Irvine) for graciously granting access to his laboratory for the isolation and preparation of the mass spectrometry samples. We also thank John Greaves (University of California, Irvine) and John Mudd (University of California, Irvine) of the mass spectrometry lab for their services in performing the mass spectrometry analysis.

Literature Cited

Andrawis, A.; Johnson, K. A.; Tien, M. Studies on compound I formation of the lignin peroxidase from *Phanerochaete chrysosporium*. *J. Biol. Chem.* **1988,** *263*, 1195−1198.

Anni, H.; Yonetani, T. Mechanism of action of peroxidases. In *Degradation of Environmental Pollutants by Microorganisms*

and Their Metalloenzymes; Sigel, H., Sigel, A., Eds.; Marcel Dekker, Inc.: New York, 1992; pp 219−241.
Bergmann, J. G.; Sanik, J., Jr. Determination of trace amounts of chlorine in naptha. *Anal. Chem.* **1957,** *29*, 241−243.
Bollag, J.-M.; Helling, C. S.; Alexander, M. 2,4-D Metabolism. *J. Agric. Food Chem.* **1968,** *16*, 826−828.
Borgmeyer, J. R.; Crawford, D. L. Production and characterization of polymeric lignin degradation intermediates from two different *Streptomyces* spp. *Appl. Environ. Microbiol.* **1985,** *49*, 273−278.
Buikema, A. L., Jr.; McGinniss, M. J.; Cairns, J., Jr. Phenolics in aquatic ecosystems: a selected review of recent literature. *Marine Environ. Res.* **1979,** *2*, 87−181.
Crawford, D. L.; Pettey, T. M.; Thede, B. M.; Deobald, L. A. Genetic manipulation of ligninolytic Streptomyces and generation of improved lignin-to-chemical bioconversion strains. *Biotechnol. Bioeng. Symp.* **1984,** *14*, 241−256.
Everse, J., Everse, K. E., Grisham, M. B., Eds. *Peroxidases in chemistry and biology*; CRC Press, Inc.: Boca Raton, FL, 1991.
Golovleva, L. A.; Zaborina, O.; Pertsova, R.; Baskunov, B.; Schurukhin, Y.; Kuzmin, S. Degradation of polychlorinated phenols by *Streptomyces rochei* 303. *Biodegradation* **1992,** *2*, 201−208.
Häggblom, M. Mechanisms of bacterial degradation and transformation of chlorinated monoaromatic compounds. *J. Basic Microbiol.* **1990,** *30*, 115−141.
Hu, Z. C.; Korus, R. A.; Venkataramu, C. R.; Crawford, R. L. Deactivation kinetics of lignin peroxidase from *Phanerochaete chrysosporium*. *Enzyme Microbiol. Technol.* **1993,** *15*, 567−574.
Kintz, P.; Tracqui, A.; Mangin, P. Accidental death caused by the absorption of 2,4-dichlorophenol through the skin. *Arch. Toxicol.* **1992,** *66*, 298−299.
Kroschwitz, J. I., Ed. *Encyclopedia of chemical technology*; John Wiley & Sons: New York, 1993.
Liu, S.-Y.; Minard, R. D.; Bollag, J.-M. Coupling reactions of 2,4-dichlorophenol with various anilines. *J. Agric. Food Chem.* **1981,** *29*, 253−257.
Minard, R. D.; Liu, S.-Y.; Bollag, J.-M. Oligomers and quinones from 2,4-dichlorophenol. *J. Agric. Food Chem.* **1981,** *29*, 250−253.
Radjendirane, V.; Bhat, M. A.; Vaidyanathan, C. S. Affinity purification and characterization of 2,4-dichlorophenol hydroxylase from *Pseudomonas cepacia*. *Arch. Biochem. Biophys.* **1991,** *288*, 169−176.
Ramachandra, M.; Crawford, D. L.; Pometto, A. L., III. Extracellular enzyme activities during lignocellulose degradation by *Streptomyces* spp.: a comparative study of wild-type and genetically manipulated strains. *Appl. Environ. Microbiol.* **1987,** *53*, 2754−2760.
Ramachandra, M.; Crawford, D. L.; Hertel, G. Characterization of an extracellular lignin peroxidase of the lignocellulolytic actinomycete *Streptomyces viridosporus*. *Appl. Environ. Microbiol.* **1988,** *54*, 3057−3063.
Segel, I. H. *Enzyme kinetics: behavior and analysis of rapid equilibrium and steady-state enzyme systems*; Wiley-Interscience: New York, 1975.
Spiker, J. K.; Crawford, D. L.; Thiel, E. C. Oxidation of phenolics and non-phenolic substrates by the lignin peroxidase of *Streptomyces viridosporus* T7A. *Appl. Microbiol. Biotechnol.* **1992,** *37*, 518−523.
Syracuse Research Corp. *Toxicological profile for 2,4-dichlorophenol*; U.S. Public Health Service: Washington, DC, 1992.
Valli, K.; Gold, M. H. Degradation of 2,4-dichlorophenol by the lignin-degrading fungus *Phanerochaete chrysosporium*. *J. Bacteriol.* **1991,** *173*, 345−352.
Wariishi, H.; Gold, M. H. Lignin peroxidase compound III. *J. Biol. Chem.* **1990,** *265*, 2070−2077.
Wentz, C. A. *Hazardous Waste Management*; McGraw-Hill Book Co.: New York, 1989.
World Health Organization. *Chlorophenols other than pentachlorophenol*; World Health Organization: Geneva, 1989.
Yee, D. C.; Wood, T. K. Elicitation of lignin peroxidase in *Streptomyces lividans*. *Appl. Biochem. Biotechnol.* **1996,** *60*, 139−149.
Yee, D. C.; Jahng, D.; Wood, T. K. Enhanced expression and hydrogen peroxide dependence of lignin peroxidase from *Streptomyces viridosporus* T7A. *Biotechnol. Prog.* **1996,** *12*, 40−46.

Accepted November 25, 1996.[⊗]

BP960091X

[⊗] Abstract published in *Advance ACS Abstracts,* January 1, 1997.